Received: 19 January 2024 | Revised: 5 February 2024 | Accepted: 8 February 2024

DOI: 10.1096/fba.2024-00015

RESEARCH ARTICLE

FASEB BioAdvances WILEY

ROCK1 deficiency preserves caveolar compartmentalization of signaling molecules and cell membrane integrity

Jianjian Shi | **Lei Wei**

Herman B Wells Center for Pediatric Research, Department of Pediatrics, School of Medicine, Indiana University, Indianapolis, Indiana, USA

Correspondence
Jianjian Shi and Lei Wei, Herman B Wells Center for Pediatric Research, Department of Pediatrics, School of Medicine, Indiana University, 1044 West Walnut Street, R4-240, Indianapolis, IN 46202-5225, USA.
Email: jishi@iu.edu and lewei@iu.edu

Abstract

In this study, we investigated the roles of ROCK1 in regulating structural and functional features of caveolae located at the cell membrane of cardiomyocytes, adipocytes, and mouse embryonic fibroblasts (MEFs) as well as related physiopathological effects. Caveolae are small bulb-shaped cell membrane invaginations, and their roles have been associated with disease conditions. One of the unique features of caveolae is that they are physically linked to the actin cytoskeleton that is well known to be regulated by RhoA/ROCKs pathway. In cardiomyocytes, we observed that ROCK1 deficiency is coincident with an increased caveolar density, clusters, and caveolar proteins including caveolin-1 and -3. In the mouse cardiomyopathy model with transgenic overexpressing Gαq in myocardium, we demonstrated the reduced caveolar density at cell membrane and reduced caveolar protein contents. Interestingly, coexisting ROCK1 deficiency in cardiomyocytes can rescue these defects and preserve caveolar compartmentalization of β-adrenergic signaling molecules including β1-adrenergic receptor and type V/VI adenylyl cyclase. In cardiomyocytes and adipocytes, we detected that ROCK1 deficiency increased insulin signaling with increased insulin receptor activation in caveolae. In MEFs, we identified that ROCK1 deficiency increased caveolar and total levels of caveolin-1 and cell membrane repair ability after mechanical or chemical disruptions. Together, these results demonstrate that ROCK1 can regulate caveolae plasticity and multiple functions including compartmentalization of signaling molecules and cell membrane repair following membrane disruption by mechanical force and oxidative damage. These findings provide possible molecular insights into the beneficial effects of ROCK1 deletion/inhibition in cardiomyocytes, adipocytes, and MEFs under certain diseased conditions.

KEYWORDS

cardiomyocyte hypertrophy, caveolae, compartmentalization, insulin signaling, mechanical injury, plasma membrane repair, ROCK1, β-adrenergic signaling

Abbreviations: AC5/6, type V/VI adenylyl cyclase; β1-AR, β1-adrenergic receptor; F-actin, actin filaments; IR, insulin receptor; IRS1, insulin receptor substrate-1; MEFs, mouse embryonic fibroblasts; MHC, α-myosin heavy chain; MLC, myosin light chain; PM, plasma membrane; ROS, reactive oxygen species; WT, wild type.

1 | INTRODUCTION

ROCKs are central regulators of the actin cytoskeleton downstream of the small GTPase RhoA.[1–8] The two ROCK isoforms, ROCK1 and ROCK2, are highly homologous with an overall amino acid sequence identity of 65%.[1–3] We previously found that ROCK1 is a key molecule in mediating apoptotic signaling in cardiomyocytes under pressure overload and in genetically induced pathological cardiac hypertrophy.[9–13] We also observed that ROCK1 deletion restores autophagic flux through reducing Beclin-1 phosphorylation in doxorubicin cardiotoxicity in global and cardiomyocyte-specific ROCK1 knockout mice.[14] Collectively, these loss-of-function studies, along with other studies in genetically modified mouse models,[15,16] have provided strong evidence that ROCK1 is a vital player for pathologic cardiac fibrosis formation and cardiomyocyte apoptotic events, though not for cardiac hypertrophy. Using mouse embryonic fibroblasts (MEFs) as an in vitro system, we observed that ROCK1 deficiency has a unique protective benefit of preserving actin cytoskeleton stability, which acts additively with antioxidant treatment to suppress excessive production of doxorubicin- or hydrogen peroxide-induced reactive oxygen species (ROS), apoptosis, and necrosis.[17–20] Moreover, ROCK1 deficiency in adipocytes and in MEFs increases insulin signaling, and adipocyte-specific ROCK1 knockout mice show modest amelioration of insulin sensitivity and insulin signaling.[21] Although the direct mechanisms underlying these beneficial effects of ROCK1 deficiency in MEF cells are largely mediated by reduced myosin light chain (MLC) phosphorylation and peripheral actomyosin contraction,[17–20] they are still incompletely understood in most of in vivo models, especially in hypertrophic cardiomyocytes[9–13] and in adipocytes.[21]

Caveolae are small bulb-shaped plasma membrane (PM) invaginations with a diameter of 50–100 nm.[22,23] They are highly abundant in mechanically stressed cells including muscle cells, adipocytes, fibroblasts, and endothelial cells. Caveolae are enriched in cholesterol and sphingolipids, as well as specific lipid binding proteins including caveolin family and cavin family. These membrane structures have been involved in many essential cellular functions and pathologies, for example, mechanoprotection is one of the major functions that serves as membrane reservoirs to buffer increased membrane tension.[24,25] The tension in the PM determines the curvature of caveolae because they flatten at high tension and invaginate to form clusters at low tension; for this reason, caveolae serve as a good tension-buffering system.[24,25] In addition, these organelles serve as signaling centers due to the enrichment of a large array of signal transduction components in those nanodomains. One of the unique features of caveolae is that they are physically linked to the actin filaments (F-actin), a major regulator of membrane tension and cell shape.[24,25] Based on the roles of RhoA and its downstream effectors including ROCKs in regulating actin cytoskeleton, we hypothesized that ROCK1 deficiency would regulate structural and functional features of caveolae in our previously established in vivo and in vitro models.

In this study, global ROCK1-deficient mice, cardiomyocyte-specific ROCK1 knockout mice, and ROCK1-deficient MEFs have been exploited for investigating the roles of ROCK1 in regulating caveolar structure and functions under physiopathological condition. Our results reveal a possible beneficial mechanism of ROCK1 deficiency in cardiomyocytes, adipocytes, and MEFs, through increasing caveolar density and clusters as well as increasing caveolar protein contents including caveolin-1 and -3, leading to the enhanced caveolar molecular signaling and the ability of maintaining PM integrity.

2 | MATERIALS AND METHODS

2.1 | Generation of mouse models

All animal experiments were conducted in accordance with the National Institutes of Health "Guide for the Care and Use of Laboratory Animals" and were approved by the Institutional Animal Care and Use Committee at Indiana University School of Medicine. Generation of ROCK1$^{-/-}$ mice was previously described.[9] In Brief, ROCK1$^{+/-}$ heterozygous mice (FVB background) were intercrossed to produce homozygous ROCK1$^{-/-}$ mice, and their wild-type (WT) littermates served as control mice. Generation of ROCK1$^{fl/fl}$ mice and cardiomyocyte-specific ROCK1 knockout mice (MHC-Cre/ROCK1$^{fl/fl}$) was previously described.[14] In brief, ROCK1$^{fl/fl}$ mice (C57BL/6 background) were crossed to the MHC-Cre mice (C57BL/6 background)[26] and bred back to ROCK1$^{fl/fl}$. Transgenic mice overexpressing Gαq in cardiomyocytes (Gαq, 25-copy line) (FVB background) have been characterized previously[27,28] and their WT littermates served as control mice. Generation of Gαq/ROCK1$^{-/-}$ mice was previously described.[10,13] In brief, the Gαq transgenic mice were mated with ROCK1$^{-/-}$ (FVB background) to generate Gαq/ROCK1$^{+/-}$ mice, which were then bred with ROCK$^{-/-}$ mice to generate Gαq/ ROCK1$^{-/-}$ mice.

2.2 | Insulin signaling analysis

Insulin signaling studies were performed on mice following overnight fasting as previously performed.[21,29,30]

Heart and white adipose tissue were harvested 6 min after intraperitoneal injection of human insulin (10 unit/kg of body weight), snap-frozen in liquid nitrogen, and stored at −80°C until analysis.

2.3 | Electron microscopy analysis

Transmission electron microscopy analysis was performed as previously described.[14,31] Ventricular specimens (cubes <3-mm square) were fixed in 2.5% glutaraldehyde, underwent sectioning and heavy metal uranyl acetate staining as contrast by the Electron Microscopy Center of Indiana University School of Medicine. At least six separate sections from each group were analyzed. Electron micrographs were acquired on a Tecnai BioTwin transmission electron microscope (Thermo Fisher Scientific, Waltham, MA, USA), equipped with an Advanced Microscopy Techniques Charge-Coupled Device (AMT CCD) camera (Advanced Microscopy Techniques, Woburn, MA, USA).

2.4 | Protein analysis

Protein samples were prepared as previously described.[10,13,14,31,32] Ventricular tissue fragments were disrupted with a PYREX® Potter-Elvehjem tissue grinder on ice in lysis buffer containing proteinase and phosphatase inhibitors (Roche, Indianapolis, IN, USA). The homogenate was centrifuged at 15,000 *g* at 4°C for 15 min, and the supernatant was saved for immunoblotting. Total protein extracts were run in equal protein amount on SDS-PAGE electrophoresis. The blots were probed with primary antibodies to ROCK1 (sc-5560), ROCK2 (sc-5561), Gαq (E-17) (sc-393), β1-adrenergic receptor (β1-AR) (sc-568), adenylyl cyclase V/VI (AC5/6) (sc-590) from Santa Cruz Biotechnology (Dallas, TX, USA), caveolin-1 (#610407), caveolin-2 (#610685), caveolin-3 (#610421) from BD Biosciences (San Jose, CA, USA), ROCK1 (#4035), insulin receptor (IR) β (#3025), p-Akt-Ser473 (#9271), p-Akt-Thr308 (#9275), Akt (#9272), p-GSK-3β-Ser9 (#9336) from Cell Signaling Technology (Danvers, MA, USA), p-IR-Tyr972 (#44800G) from Invitrogen. All blots were normalized to GAPDH (ABS16; MilliporeSigma, Burlington, MA, USA) or to actin (MABT523; MilliporeSigma).

2.5 | Preparation of caveolae-enriched cell membrane fractions

Tissues (Ventricular, adipose) or MEFs were fractionated using a detergent-free and high pH (sodium bicarbonate, pH 11) method and with a discontinuous sucrose gradient.[33] Tissue fragments were disrupted with a PYREX® Potter-Elvehjem tissue grinder on ice in 500 mM sodium carbonate, pH 11.0, then sonicated by three cycles of 20-s bursts of sonication and 1 min of incubation on ice. Equivalent amounts of protein from each homogenate (approximately 10 mg of total protein in 2 mL of lysis buffer) were mixed with 2 mL of 90% sucrose in MES-buffered saline (25 mM MES and 150 mM NaCl, pH 6.0) to form 45% sucrose and loaded at the bottom of an ultracentrifuge tube. A discontinuous sucrose gradient was generated by layering 4 mL of 35% sucrose prepared in MES-buffered saline and 250 mM sodium carbonate, followed by 4 mL of 5% sucrose also in MES-buffered saline/sodium carbonate. Gradients were centrifuged at 280,000 *g* using a Beckman SW 41Ti rotor for 16–20 h at 4°C. At the completion of the centrifugation, samples were removed in 1-mL aliquots to form 12 fractions, starting from the top of the gradient. Fraction-4 through -6 (caveolar fractions) are buoyant membrane fractions enriched in lipids, caveolins, and proteins associated with caveolins. Protein content in each fraction was measured. For immunoblotting, an equal volume of each fraction was subjected to SDS-PAGE electrophoresis, as this is convention for immunoblots of sucrose density gradient fractions. Cholesterol levels in fractions were measured with the Amplex Red Cholesterol Assay kit (Invitrogen, Waltham, Massachusetts, USA). Of note, to compare the caveolar protein content and caveolar levels of caveolins and signaling molecules between different genotypes, samples from different genotypes were prepared together and sucrose density gradient was performed simultaneously from the equivalent amounts of total protein for each genotype. For immunoblotting, the sucrose density gradient fraction- 4 to -6 were combined and were run in equal volume for each genotype on SDS-PAGE electrophoresis.

2.6 | Cell membrane injury and repair assays

Wild-type and ROCK1-deficient MEF cells were prepared from WT and ROCK1$^{-/-}$ embryos as previously described.[17] Cells were cultured in a 24-well plate, 1×10^5 cells/well, and were treated at ~80% confluence with scraping injury, bulk cell membrane injury by glass beads or treatment with doxorubicin. To perform scraping injury, the culture media was removed and replaced with 0.5 mL of membrane repair buffer (HBSS, 2 mM calcium acetate)/well, followed by gently scraping attached cells with a plastic cell scraper, and then 0.5 mL trypan blue (#T8154; MilliporeSigma)/well was added after recovery time of 0 to 300 s. Cells were collected and counted immediately after

adding trypan blue for trypan blue-positive and -negative cells. The ratio of cells that failed to be repaired is determined by quantitative analyses of trypan blue-positive and total cells (sum of trypan blue-positive and -negative cells). The samples were prepared in quadruplicate and at least 100 cells were analyzed for each well. At least three independent experiments were analyzed.

To perform bulk cell membrane injury by glass beads, the culture media was removed and replaced with 0.5 mL/well of fresh media containing Hoechst 33342 for 20 min to stain cell nuclei. The Hoechst 33342 containing media was then removed and replaced with 0.5 mL of membrane repair buffer containing 0.12 g of glass bead (MilliporeSigma). Cells were injured by rolling glass beads over the cells by rotating the bead-containing media in wells. The bead-containing media was then removed and replaced with 0.5 mL of membrane repair buffer, then letting cells to heal for 5 min. Unrepaired cells were stained by adding 0.25 mL of membrane repairing buffer containing 2 nM of Sytox Green (Life Technologies, Carlsbad, CA, USA)/well for 5 min, and then determined by imaging and quantitative analysis using Cytation 3 (BioTek Instruments, Winooski, VT, USA) as previously described.[17,20] The ratio of cells that failed to be repaired is determined by quantitative analyses of green nuclei (Sytox Green positive cells) and blue nuclei (Hoechst 33342 staining cells). The samples were prepared in duplicate and at least 5000 cells were analyzed for each well. At least five independent experiments were analyzed. To perform the treatment of doxorubicin alone or in combination with bead injury, cells were treated with 3 μM of doxorubicin (MilliporeSigma) in culture media for 4 h. The drug containing media was then removed and replaced with 0.5 mL of fresh culture media containing Hoechst 33342 for 20 min; to add mechanical injury, bead injury was followed as described above.

2.7 | Statistical analysis

Data are reported as mean ± SE. Comparisons between groups were analyzed by student's *t*-test or ANOVA as appropriate, with $p < 0.05$ considered as significant.

3 | RESULTS

3.1 | Global ROCK1 deletion increases caveolae protein content and caveolin levels in caveolae at the cell membrane

Caveolae shown as a subset of membrane lipid rafts were morphologically identified in the 1950s; they are bulb-shaped, 50- to 100-nm invaginations of the PM.[34,35] Caveolae are membrane regions enriched in particular lipids (e.g., cholesterol and sphingolipid), serving as membrane reservoirs and are capable of changing shapes in response to membrane tension altering. Caveolins are key structural determinants of the caveolar membrane coat and are important for forming and stabilizing the bulb-shaped membrane invagination. There are three isoforms of caveolin, caveolin-1, caveolin-2, and caveolin-3; caveolin-1 is the predominant isoform, caveolin-3 is the striated muscle-specific isoform, and caveolin-2 is found in hetero-oligomers with caveolin-1 and caveolin-3.[36] Caveolins interact via their scaffolding domain with many different signaling molecules, which are compartmentalized in caveolae. Importantly, caveolae are physically associated to actin cytoskeleton which regulate caveolar organization (Figure 1A). To investigate whether ROCK1-mediated actin cytoskeletal changes modulate caveolar organization and function, we first examined the effects of ROCK1 deletion on cardiac caveolar microdomain structure and function on 12-week-old WT and ROCK1$^{-/-}$ mice (Figure 1). We confirmed that caveolae presented in subcellular fractionations with discontinuous sucrose gradient centrifugation, a most widely used biochemical technique in caveolae study, usually with nonionic detergents or high pH.[33] We implemented high pH sucrose fractionation after disrupting cellular integrity of ventricular homogenates and the equal amounts of proteins from WT and ROCK1$^{-/-}$ were loaded simultaneously. Our result shows a low but detectable level of ROCK1, ROCK2, and RhoA cofractionating with caveolin-1 and caveolin-3 in lipid raft fractions of ventricular tissues of WT hearts (Figure 1B), and their distribution pattern in ROCK1$^{-/-}$ hearts was like the WT hearts except the absence of ROCK1 (data not shown). RhoA, ROCK1, and ROCK2 are mainly present in the heavy fractions (fractions 9 through 12). Interestingly, in ROCK1$^{-/-}$ ventricular tissues, we observed a significant increase (around 30%) in caveolar protein content (Figure 1C,D), but not in caveolar cholesterol content (Figure 1E,F). In addition, both caveolin-1 and caveolin-3 protein expressions were increased in lipid raft fractions of ROCK1$^{-/-}$ mice, without changes of their levels in ventricular homogenates (Figure 1G). Of note, in order to normalize the results for rationally comparison, the western blots evaluating the total ventricular homogenates were run in equal protein amount; nonetheless, sucrose density gradient evaluating the molecules' location and level in gradient fractions were loaded in equal volume.

3.2 | Global ROCK1 deletion increases caveolar density and clusters at the cell membrane

The biochemical finding described above is supported by the morphological analysis through electron microscopy (Figure 2). Transmission electron microscopy revealed increased numbers of clusters of caveolae in

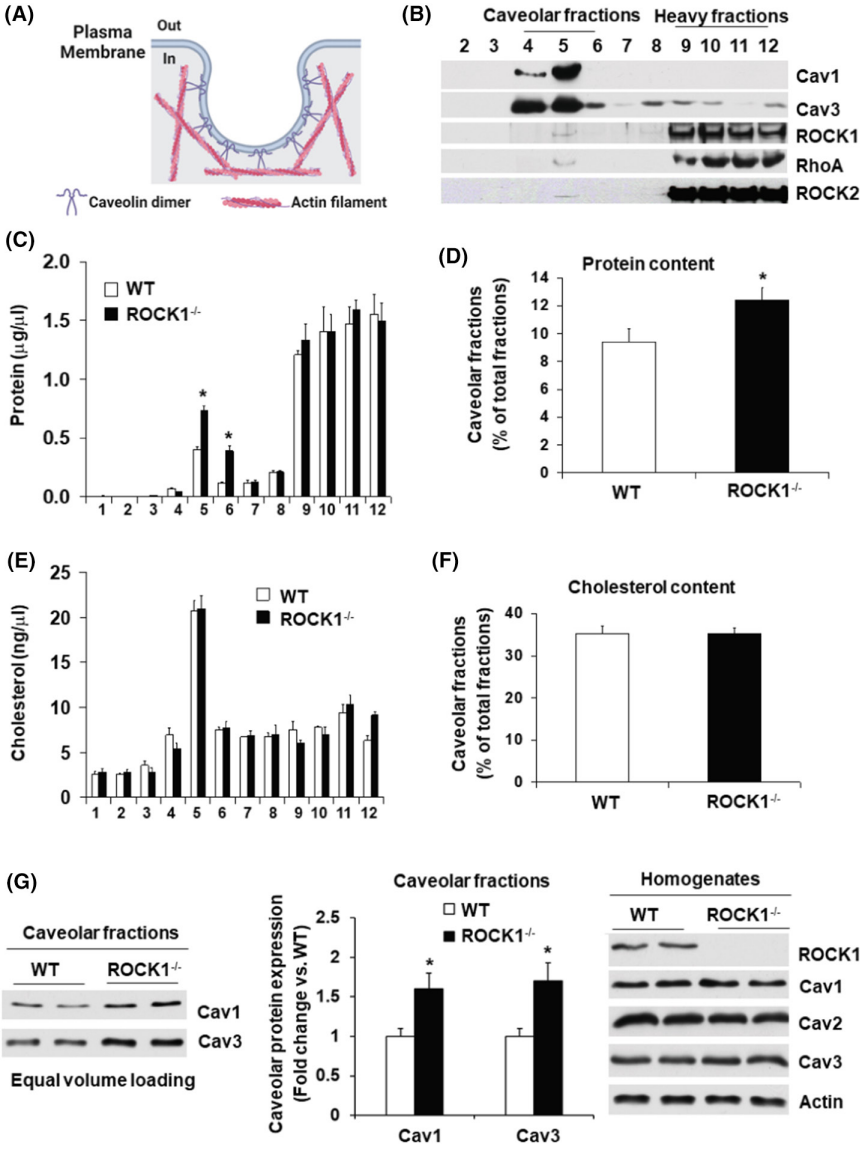

FIGURE 1 ROCK1 deletion increases caveolae protein content and caveolin levels in caveolae. (A) Schematic overview of caveolae and its links to the actin filaments. (Fig. is created with BioRender.com). (B) Representative images of Western blots of sucrose density fractions 2–12 from ventricular tissues of 12-week-old mice, showing a low but detectable level of ROCK1, ROCK2, and RhoA cofractionating with caveolin-1 (Cav1) and caveolin-3 (Cav3) in lipid raft fractions. (C, D) Protein concentration in each of all 12 sucrose density fractions (C) and in pooled lipid raft fraction- 4 through -6 (caveolar fractions) expressed as the percent of total protein accumulated in all 12 fractions (D). Increased protein content was observed in caveolar fractions from ROCK1 deficient ventricular tissues versus WT. (E, F) Cholesterol concentration in each of the sucrose density fractions 1 through 12 (E) and in pooled lipid raft fraction-4 through -6 (caveolar fractions) (F), showing no increased caveolar cholesterol content in ROCK1 deficient ventricular tissues versus WT. (G) Western blots of caveolar fractions (left panel) and ventricular homogenates (right panel), showing increased caveolin protein expression in the caveolar fractions, but not in the ventricular homogenates of ROCK1 deficient ventricular tissues versus WT. $N = 4–6$ in each group. $^*p < 0.05$ versus WT mice.

ROCK1-deficient cardiomyocytes compared to the numbers in WT cardiomyocytes, which showed predominantly single caveolae (Figure 2A). Moreover, ROCK1 deletion increased the density but not the size of caveolae in cardiomyocytes (Figure 2B,C). However, increased caveolar protein content, caveolar density and clusters observed in ROCK1$^{-/-}$ hearts do not demonstrate obvious effect on cardiac physiology in ROCK1$^{-/-}$ mice, which exhibit normal phenotype as previously characterized.[9]

3.3 | Cardiomyocyte-specific ROCK1 deletion mimics systemic knockout phenotype

To further confirm that ROCK1 is involved in the regulation of caveolar microdomains in cardiomyocytes, we performed analyses on MHC-Cre/ROCK1$^{fl/fl}$ mice (Figure 3). We observed a significant increase in caveolar protein content (Figure 3A) in MHC-Cre/ROCK1$^{fl/fl}$ ventricular

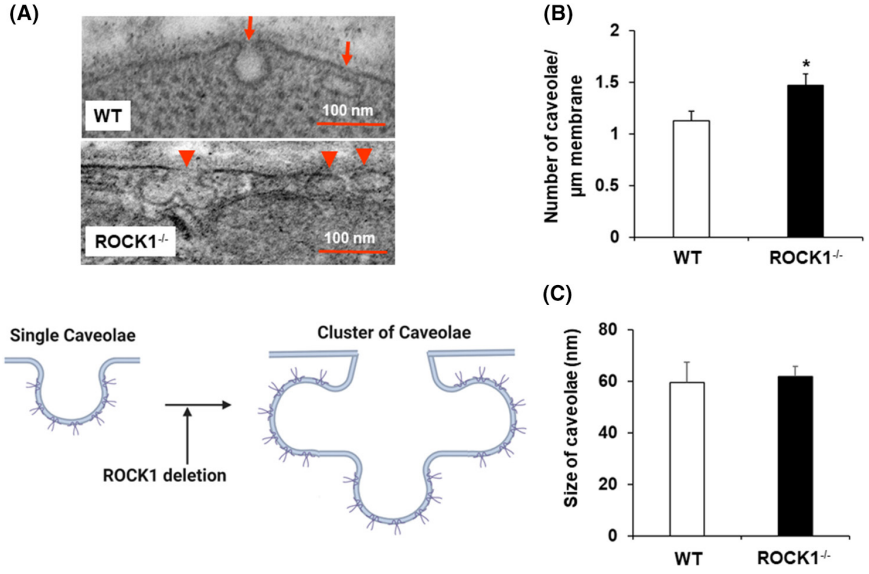

FIGURE 2 ROCK1 deletion increases caveolar density and clusters in cardiomyocytes. (A) Representative transmission electron microscopy images of WT and ROCK1 deficient hearts of 12-week-old mice (upper panel), and schematic overview of different organizational forms of caveolae and conditions regulating the transition between them (lower panel, Fig. is created with BioRender.com). ROCK1 deficient cardiomyocytes showed increased numbers of clusters of caveolae (red arrow heads) compared to WT cardiomyocytes which showed predominantly single caveolae (red arrows). (B, C) Quantification of caveolae density normalized to membrane length (B) and caveolae size (C), showing increased caveolae density in ROCK1 deficient cardiomyocytes. $N = 20–25$ micrographs from three mice per genotype. $^*p < 0.05$ versus WT mice.

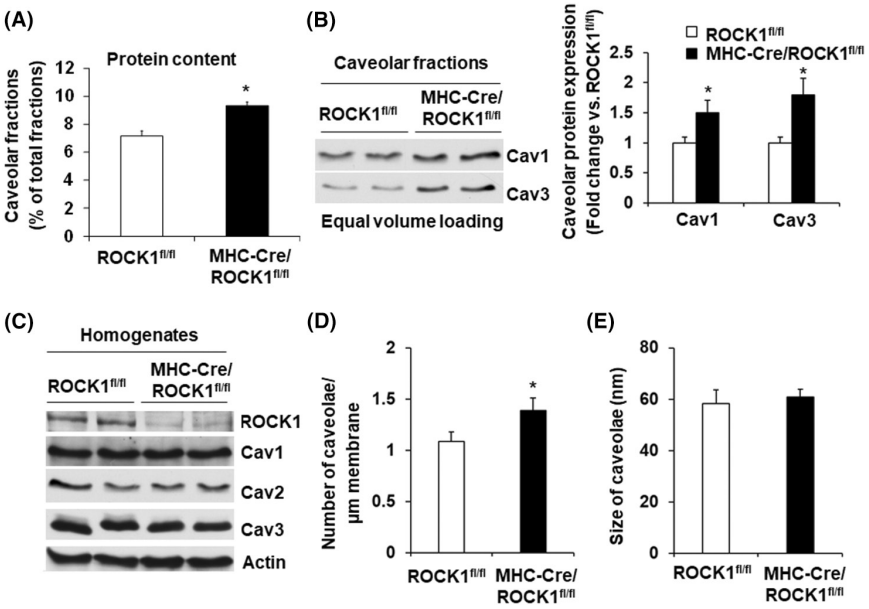

FIGURE 3 Cardiomyocyte-specific ROCK1 deletion mimics systemic knockout phenotype. (A) Protein content in caveolar fractions (pooled fractions 4–6) from sucrose density fractions of 3-week-old MHC-Cre/ROCK1$^{fl/fl}$ and ROCK1$^{fl/fl}$ mice, showing increased protein content in caveolar fractions in cardiomyocyte-specific ROCK1 deficient ventricular tissues. (B, C) Western blots of caveolar fractions (B) and ventricular homogenates (C), showing increased caveolin protein expression in caveolar fractions, but not in ventricular homogenates of cardiomyocyte-specific ROCK1-deficient ventricular tissues. $N = 4–6$ in each group. (D, E) Quantification of caveolae density normalized to membrane length (D) and caveolae size (E), showing increased caveolae density in MHC-Cre/ROCK1$^{fl/fl}$ cardiomyocytes. $N = 20–25$ micrographs from three mice per genotype. $^*p < 0.05$ versus ROCK1$^{fl/fl}$ mice.

tissues, like in ROCK1$^{-/-}$ hearts. Both caveolin-1 and caveolin-3 protein expressions were increased in lipid raft fractions of MHC-Cre/ROCK1$^{fl/fl}$ hearts (Figure 3B,C). Transmission electron microscopy also revealed increased caveolae density in MHC-Cre/ROCK1$^{fl/fl}$ cardiomyocytes (Figure 3D,E). Of note, these experiments were performed on young MHC-Cre/ROCK1$^{fl/fl}$ mice of 3-week-old age to avoid cardiotoxicity which can be detected from 3 month of age in the MHC-Cre mice.[37] MHC-Cre mice of 1- to 3-week-old were examined to confirm no nonspecific toxic effects of Cre activity (data not shown). Together, these results support a novel role of ROCK1 in regulating caveolar organization and protein contents in cardiomyocytes. To explore the functional significance of this discovery, we further examined the effects of ROCK1 deficiency on caveolar organization and functions in several in vivo and in vitro models as described below.

3.4 | ROCK1 deficiency prevents down-regulation of caveolae protein content and caveolae density induced by Gαq overexpression

Cardiac hypertrophy is manifested by heart muscle thickening attributed to the size of cardiomyocyte increasing, which ultimately leads to progressive heart failure. Reported studies have established caveolae-mediated mechanoprotection and adaptive hypertrophic signaling in pathological cardiac hypertrophy.[38,39] We have previously found that ROCK1-deficient mice exhibit improved cardiac functions, reduced apoptosis and fibrosis in several pathologic mouse models, for example, under pressure overload and in transgenic mice overexpressing Gαq in cardiomyocytes (a genetically induced pathological cardiac hypertrophy model).[9–13] To further explore the cellular and molecular mechanisms underlying the cardioprotective effects of ROCK1 deficiency, we examined caveolar organization and caveolar protein content in 12-week-old Gαq and Gαq/ROCK1$^{-/-}$ mice (Figure 4A). The sucrose fractionation was performed simultaneously with equal amounts of protein loading prepared from WT, ROCK1$^{-/-}$, Gαq, and Gαq/ROCK1$^{-/-}$ ventricular homogenates. We observed that both caveolar protein content and caveolae density in Gαq hearts were noticeably reduced compared with the WT hearts (Figure 4B–E). Importantly, Gαq/ROCK1$^{-/-}$ hearts showed an increase in caveolar protein content by around 70% compared with Gαq hearts (Figure 4B), associated with a significant increase in the density and size of caveolae (Figure 4D,E). Alike ROCK1$^{-/-}$ cardiomyocytes (Figure 2A), Gαq/ROCK1$^{-/-}$ cardiomyocytes showed increased clusters of caveolae, while Gαq cardiomyocytes showed predominantly single caveolae, and some with more flattened shape (Figure 4C,F). These differences in the caveolar organization between the Gαq and Gαq/ROCK1$^{-/-}$ cardiomyocytes support a potentially novel cardioprotective mechanism that ROCK1 deficiency enhances caveolar protective effects in hypertrophic cardiomyocytes (Figure 4F).

3.5 | ROCK1 deficiency prevents downregulation of caveolar β-adrenergic signaling molecules induced by Gαq overexpression

Caveolins interact with many different signaling molecules via their scaffolding domain. Such signaling components include β1-AR, β2-AR, and downstream effectors including AC5/6 (Figure 5A). We previously reported that ROCK1 deletion prevents downregulation of AC5/6 expression, which contributes to the impaired β-adrenergic signaling in Gαq mice.[10,13] The mechanisms underlying the downregulation of AC5/6 in Gαq hearts is not clear and appears to be a post-translational event as the mRNA levels were not affected. To further explore the mechanisms of ROCK1 deficiency on the preserved β-adrenergic response in Gαq/ROCK1$^{-/-}$ mice, we measured caveolar expressions of caveolins, β1AR and AC5/6 in Gαq and Gαq/ROCK1$^{-/-}$ hearts (Figure 5). The distribution of β1AR and AC5/6 on sucrose density gradient fractions in WT hearts (Figure 5A) was consistent with previously reported,[40] and their distribution patterns for Gαq, ROCK1$^{-/-}$ and Gαq/ROCK1$^{-/-}$ hearts were similar to the WT hearts (data not shown). The caveolar expressions of caveolin-1, caveolin-3, β1AR and AC5/6 were all reduced in the Gαq hearts (Figure 5B), which support that reduced caveolar proteins including caveolins and key β-adrenergic signaling molecules contribute to the impaired β-adrenergic signaling in Gαq hearts, and the rationale may be explained by the co-recruitment of these molecules into caveolae can enhance their interaction. The downregulation of caveolar expression of caveolins, β1AR and AC5/6 was completely rescued in Gαq/ROCK1$^{-/-}$ hearts (Figure 5B) supporting that ROCK1 deficiency preserves β-adrenergic response through maintaining caveolins and β-adrenergic signaling molecules in caveolae. In addition, caveolar expression of eNOS that is another caveolar enriched protein was parallel with β1AR and AC5/6 downregulation in Gαq hearts, but it was restored in Gαq/ROCK1$^{-/-}$ hearts (Figure 5). Consistent with our previous observation,[10,13] although the total expression level of AC5/6 was reduced in Gαq hearts, it can be rescued in Gαq/ROCK1$^{-/-}$ hearts; however, the total protein

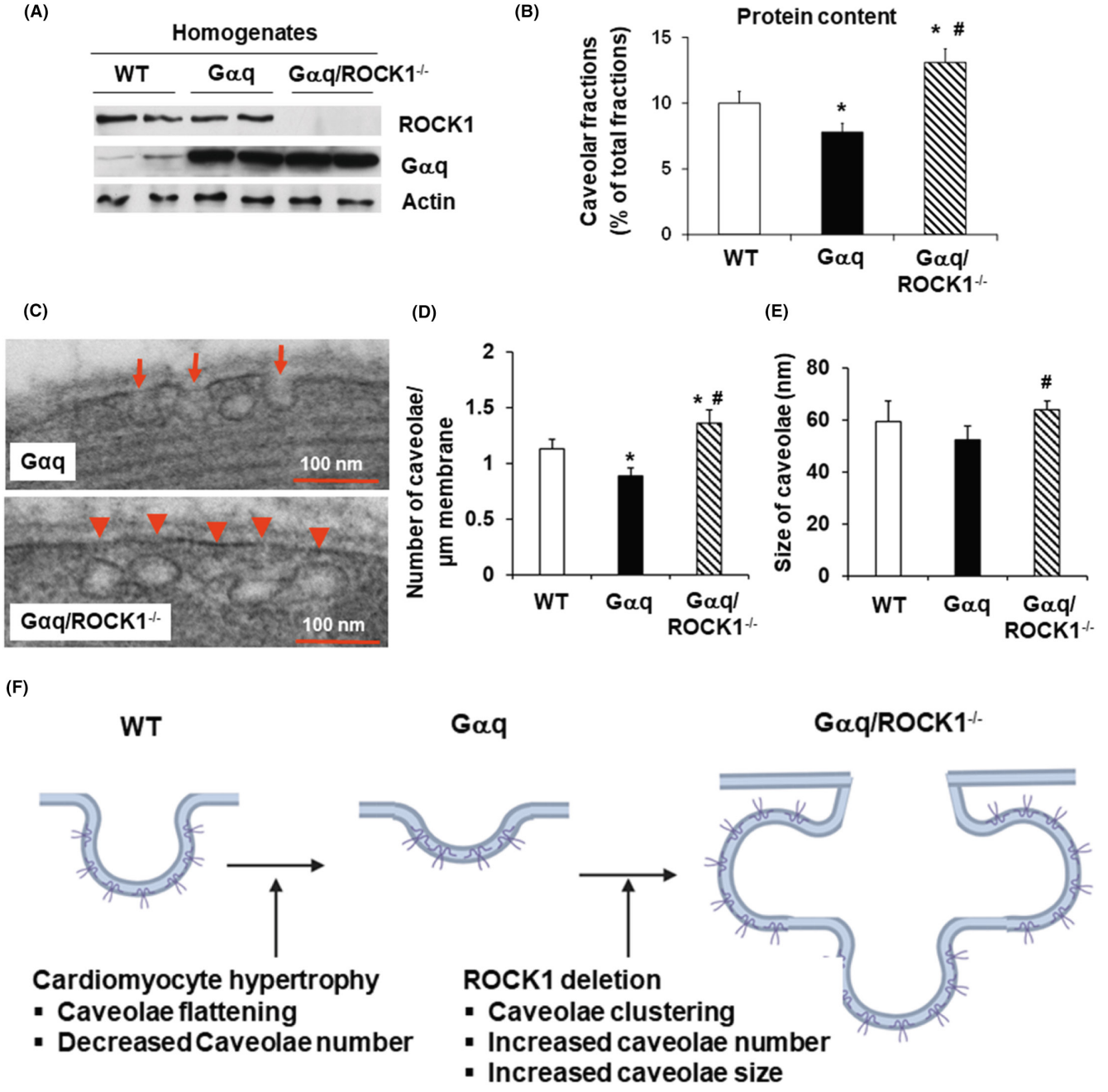

FIGURE 4 Pathological cardiac hypertrophy induced by Gαq overexpression reduces caveolae protein content and caveolae density which are prevented by ROCK1 deletion. (A) Representative images of Western blot analysis of Gαq, ROCK1, and Actin in ventricular homogenates from 12-week-old mice. (B) Protein content in caveolar fractions (pooled fractions 4–6) from sucrose density fractions showing decreased caveolar protein content in Gαq hearts (decreased by 22.3% compared to WT) and increased caveolar protein content in Gαq/ROCK1$^{-/-}$ (increased by 68.6% compared to Gαq). (C) Representative transmission electron microscopy images of Gαq and Gαq/ROCK1$^{-/-}$ hearts of 12-week-old mice. Gαq/ROCK1$^{-/-}$ cardiomyocytes showed increased numbers of clusters of caveolae (red arrow heads) compared to Gαq cardiomyocytes which showed predominantly single caveolae (red arrows). (D, E) Quantification of caveolae density normalized to membrane length (D) and caveolae size (E), showing reduced caveolae density in Gαq cardiomyocytes compared to WT cardiomyocytes and increased both caveolae density and size in Gαq/ROCK1$^{-/-}$ cardiomyocytes compared to Gαq cardiomyocytes. $N = 20–25$ micrographs from three mice per genotype. *$p < 0.05$ versus WT mice. $^{\#}p < 0.05$ versus Gαq. (F) Schematic overview of different organizational forms of caveolae and conditions regulating the transition between them. (Fig. is created with BioRender.com).

expressions of other caveolae enriched proteins such as caveolin-1, caveolin-3, β1AR and eNOS were unaltered in Gαq and Gαq/ROCK1$^{-/-}$ hearts (Figure 5C), supporting that Gαq overexpression or ROCK1 deletion only changes the caveolar localization of these molecules, but not their protein expression.

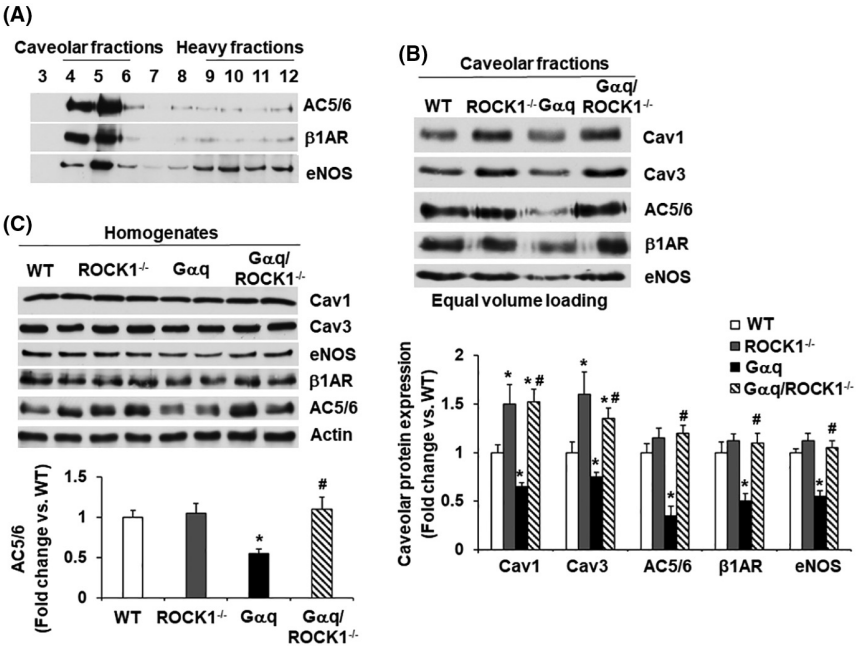

FIGURE 5 Pathological cardiac hypertrophy induced by Gαq overexpression reduces the protein expression of caveolins, eNOS and β-adrenergic signaling molecules (AC5/6, β1AR) in caveolae which are prevented by ROCK1 deletion. (A) Representative images of Western blots of sucrose density fractions 2–12 from ventricular tissues of 12-week-old WT mice, showing a preferential caveolar localization of AC5/6, β1AR and eNOS. (B) Representative images of Western blots of caveolar fractions (pooled sucrose density fractions 4–6) showing reduced caveolar expressions of caveolin-1 (Cav1), caveolin-3 (Cav3), AC5/6, β1AR and eNOS in Gαq hearts compared to WT hearts. The caveolar expressions of these proteins were preserved in Gαq/ROCK1$^{-/-}$ hearts. (C) Representative images of Western blots of ventricular homogenates showing reduced AC5/6 expression but not caveolin-1, caveolin-3, β1AR and eNOS in Gαq hearts compared to WT hearts. ROCK1 deletion prevented down-regulation of AC5/6. $N = 4–6$ in each group. *$p < 0.05$ versus WT mice. $^{\#}p < 0.05$ versus Gαq.

3.6 | ROCK1 deficiency enhances IR activation in heart and in caveolar fractions

ROCK1 deficiency not only plays roles through modulating β-adrenergic signaling molecules in caveolae, but also modulates insulin signaling through affecting proper compartmentalization of insulin signaling molecules as IR is mainly localized in caveolae.[41–43] To examine the effects of ROCK1 deficiency on cardiac insulin signaling, we assessed the ability of insulin in activating IR and the level of activated IR in caveolae in ROCK1$^{-/-}$ mice (Figure 6). Loss of ROCK1 caused a significant increase in insulin-stimulated IR tyrosine phosphorylation in ROCK1$^{-/-}$ hearts compared with WT hearts (Figure 6A). In addition, IR downstream signaling such as insulin-stimulated Akt and GSK3 phosphorylation was markedly enhanced in ROCK1$^{-/-}$ hearts (Figure 6A). These effects are largely due to increased IR tyrosine phosphorylation, which is the initiating component of insulin signaling cascade when IR is stimulated. The distribution of activated IR on sucrose density gradient fractions of WT hearts (Figure 6B) was consistent with previously reported preferential caveolar localization[41–43] and a similar distribution pattern was observed with ROCK1$^{-/-}$ hearts (data not shown). Moreover, the level of the activated IR in caveolae was increased in ROCK1$^{-/-}$ hearts compared with WT hearts, similarly to that of caveolin-3 (Figure 6C), supporting that ROCK1 deficiency improves cardiac insulin signaling through enhancing caveolar IR localization and activation.

3.7 | ROCK1 deficiency increases the expressions of caveolin-1 and activated IR in caveolae of adipose tissues

Besides the enhanced IR activation observed in heart, we have previously reported that ROCK1 deficiency enhances insulin signaling in adipocytes and MEFs through increased IR activation.[21] Of note, increased insulin-stimulated IR tyrosine phosphorylation was confirmed in the adipose tissues of global ROCK1-deficient mice, adipocyte-specific ROCK1 knockout mice, and in ROCK1-deficient MEFs, associated with increased phosphorylation of downstream molecules including insulin receptor substrate-1 (IRS1), Akt, and GSK.[21] However, the mechanisms underlying the enhanced IR activation in ROCK1-deficient adipose tissue and MEFs have not been defined.[21] Following this previous

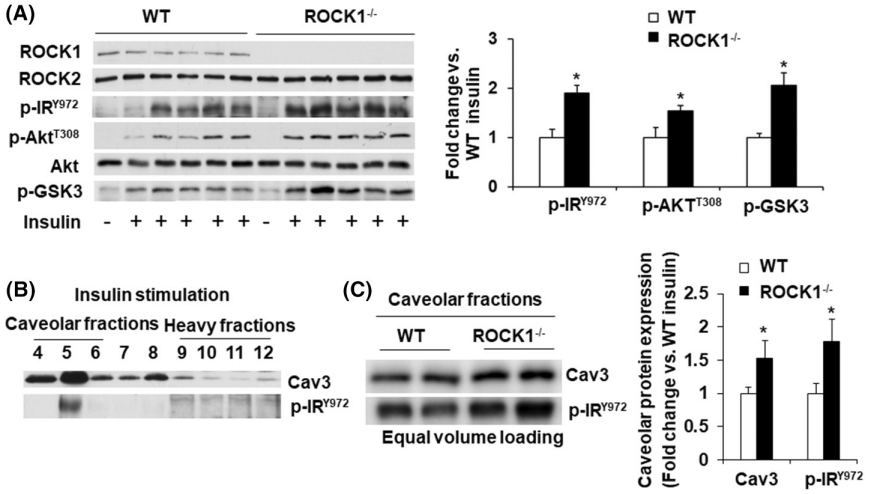

FIGURE 6 ROCK1 deficiency in mice results in enhanced IR activation in heart and increased caveolar expressions of p-IR^{Y972}. (A) Representative of Western blots of ventricular homogenates WT and ROCK1$^{-/-}$ mice. After an overnight fast, six-month-old female mice were injected intraperitoneally with saline or 10 units/kg insulin. Six min later, heart was removed. Insulin-stimulated receptor phosphorylation (p-IR^{Y972}), Akt and GSK3 phosphorylation were increased in ROCK1$^{-/-}$ heart compared to WT heart. (B) Representative images of Western blots of sucrose density fractions 4–12 from ventricular tissues of six-month-old WT mice, showing a preferential caveolar localization of p-IR^{Y972}. (C) Western blots of caveolar fractions (pooled sucrose density fractions 4–6), showing increased caveolin-3 (Cav3) and p-IR^{Y972} protein expression in the caveolar fractions of ROCK1 deficient ventricular tissues. $N = 4–6$ in each group. *$p < 0.05$ versus WT mice.

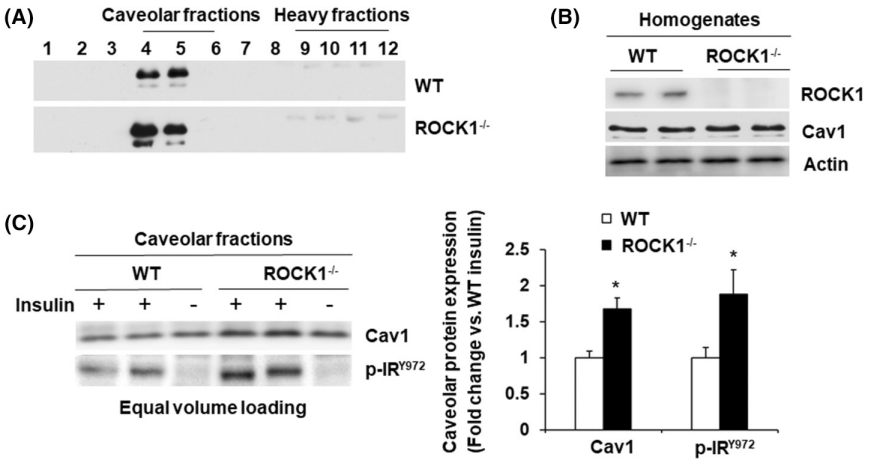

FIGURE 7 ROCK1 deficiency in mice results in enhanced IR activation in adipose tissue and increased caveolar expressions of caveolin-1 (Cav1) and p-IR^{Y972}. (A) Representative images of Western blots of sucrose density fractions 1–12 from white adipose tissues of six-month-old WT and ROCK1$^{-/-}$ mice, showing enriched caveolin-1 expression in the sucrose fractions 4 and 5. (B) Representative of Western blots of adipose homogenates WT and ROCK1$^{-/-}$ mice showing similar protein expression of caveolin-1 in the adipose tissue of WT and ROCK1$^{-/-}$ mice. (C) Western blots of caveolar fractions (pooled sucrose density fractions 4–5), showing increased caveolin-1 and p-IR^{Y972} protein expression in the caveolar fractions of ROCK1 deficient adipose tissues. After an overnight fast, six-month-old female mice were injected intraperitoneally with saline or 10 units/kg insulin. Six min later, adipose tissue was removed and subjected to sucrose density gradient analysis. $N = 4–6$ in each group. *$p < 0.05$ versus WT mice.

study, we examined caveolar and total levels of caveolin-1 in WT and ROCK1$^{-/-}$ adipose tissues (Figure 7) and MEFs (Figure 8). In the WT and ROCK1$^{-/-}$ adipose tissues, only fractions 4 and 5 from sucrose density fractions were enriched in caveolin-1, which is different from heart showing that fractions 4, 5 and 6 were enriched in caveolin-1 (Figure 7A), it is most likely due to lipid content difference in adipose tissue versus in heart tissue. The total level of caveolin-1 was unaltered in the adipose tissue (Figure 7B), but caveolin-1 and activated IR expressions in caveolae were increased in ROCK1$^{-/-}$ mice when compared to WT mice (Figure 7C), supporting that ROCK1 deficiency

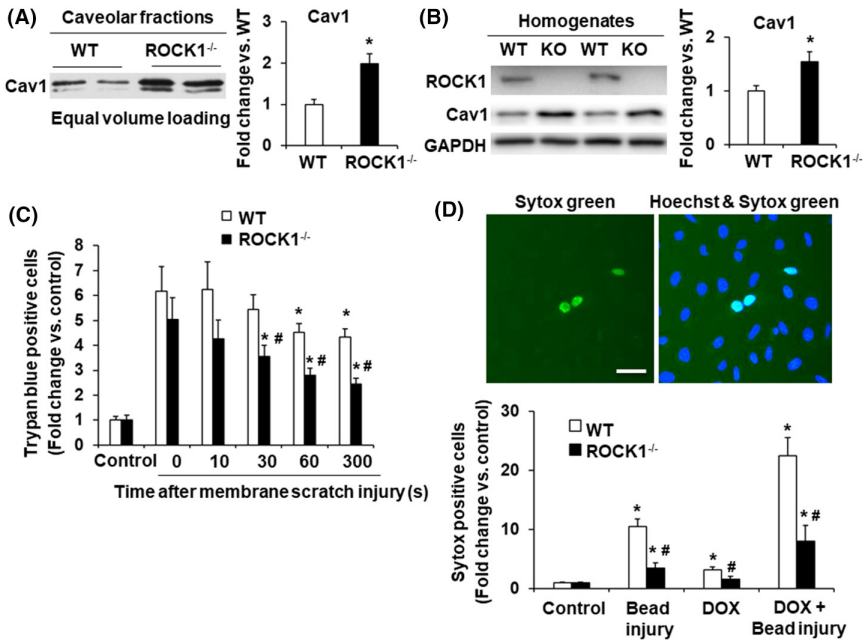

FIGURE 8 ROCK1 deficiency in MEFs results in increased caveolar and total protein expressions of caveolin-1 (Cav1), and increased cell membrane repair ability following membrane disruption. (A, B) Western blots of caveolar fractions (pooled sucrose density fractions 4–6) (A) and homogenates (B) of WT and ROCK1$^{-/-}$ MEFs, showing increased caveolin-1 in caveolar fractions and in cell homogenates of ROCK1$^{-/-}$ MEFs. $N = 4$–6 in each group. (C) Unrepaired cells measured by trypan blue-positive cells at indicated times after scrape injury, expressed as fold change versus baseline which was arbitrarily set at 1 (lower panel). At least 1200 cells were analyzed for each condition. *$p < 0.05$ versus the time point immediately after scrape injury of the same genotype. #$p < 0.05$ versus WT under the same treatment condition. (D) Representative images of Sytox Green (green) and Hoechst 33342 staining (blue) of ROCK1$^{-/-}$ MEFs treated with glass beads (upper panel). Bar, 100 μm. Cells were treated with glass beads, doxorubicin (DOX) at 3 μM for 4 h, or doxorubicin at 3 μM for 4 h followed by the treatment with glass beads (lower panel). Unrepaired cells measured by Sytox Green positive cells, expressed as fold change versus baseline which was arbitrarily set at 1. At least 20,000 cells were analyzed for each condition. *$p < 0.05$ versus control of the same genotype. #$p < 0.05$ versus WT under the same treatment condition.

improves adipose insulin signaling through enhancing caveolar IR localization and activation. In MEFs, the caveolar and total levels of caveolin-1 were both increased in ROCK1$^{-/-}$ cells compared to WT cells (Figure 8A,B), supporting that increased caveolar IR localization/activation is a shared mechanism for the increased insulin signaling observed in heart, adipose tissue and MEFs.

3.8 | ROCK1 deficiency in MEFs increases cell membrane repair ability following mechanical injury and doxorubicin-induced cytotoxicity

In addition to fostering appropriate environments for signaling molecules, caveolae are involved in maintaining cell membrane integrity in the face of external stresses including mechanical and oxidative damages. To examine the acute consequences of ROCK1 deficiency on membrane resealing following mechanical damage, we first applied scraping injury via a standard cell wounding method[44] on ROCK1$^{-/-}$ and WT MEFs to assess the kinetic process of membrane resealing. After scraping injury, trypan blue was added after recovery time of 0 to 5 min, allowing the wounded cells that failed to be resealed to be identified by trypan blue uptake. A significant reduction in trypan blue positive cells was observed in ROCK1$^{-/-}$ MEFs at 0.5, 1 or 5 min consistent with improved cell membrane repair when compared to WT MEFs (Figure 8C). We validated this finding by implementing glass-bead injury and allowing cells 5 min for resealing. The unrepaired cells indicated by Sytox Green uptake were imaged and counted automatically by Cytation 3 (Figure 8D), the similar results were obtained as noted in scrape-injury study. Thus, ROCK1$^{-/-}$ MEFs, compared to WT MEFs, have shown resealing cell membrane more rapidly after mechanical wounds, consistent with their increased caveolar density and clusters at the cell membrane. Of note, both scrape-injury and glass-bead-injury followed by measuring the uptake of membrane impermeable dye from 30 s to 5 min have been widely used to measure membrane resealing after mechanical injuries.[44,45]

We have previously reported that ROCK1 deficiency can reduce doxorubicin-induced ROS generation, apoptosis and necrotic cell death.[19,20] To examine whether ROCK1

deficiency improves cell membrane resealing following both mechanical and oxidative damages, we applied glass-bead injury to doxorubicin treated ROCK1$^{-/-}$ and WT MEFs. Prior to glass-bead injury, doxorubicin treatment was performed at 3 μM for 4 h that is an established condition to observe increased ROS production, while both apoptosis and necrosis occur largely at 16–24 h.[19,20] The number of unrepaired cells following bead injury was doubled by additional doxorubicin treatment indicating that both injuries synergistically induce cell membrane damages (Figure 8D). It is possible that oxidative damages caused by doxorubicin treatment could result in a greater susceptibility of the cell membrane to mechanical damages in addition to inhibiting cell membrane resealing. The observations that ROCK1 deficient MEFs showed remarkable reduction of unrepaired cell number under all tested conditions (Figure 8D) suggest a beneficial effect of ROCK1 deletion in preserving cell membrane integrity of MEFs following mechanical and oxidative damages.

4 | DISCUSSION

In current study, we discovered that ROCK1 deficiency is accompanied with increased caveolins and protein contents in caveolae of cardiomyocytes, adipose tissue, and MEFs leading to improved caveolar molecular signaling and increased mechanoprotection. Caveolae are bulb-shaped PM invaginations, the lipids, and proteins formed vesicle microdomains, which can flatten into the membrane to release mechanical stress applied on the cells.[46] Although the molecular mechanisms underlying the diverse cellular functions of caveolae remain to be uncovered, current growing molecular understanding of caveolae formation is revealing new insights into their physiopathology roles in regulating multiple processes in the cell membrane, including the structure modulation to benefit signaling complex formation and to adapt the tension alteration applied on cell membrane under diverse disease conditions.[47,48] An important feature of caveolae is that they are physically linked to the actin cytoskeleton,[24,25] therefore, possibly regulated by RhoA/ROCKs pathway; of note, as a highly dynamic network, the cytoskeleton is relating to diverse biological functions.

The major findings of the current study include (1) in cardiomyocytes, ROCK1 deficiency is associated with increased caveolar density and clusters, as well as caveolar protein contents including caveolin-1 and -3. Interestingly, the total protein level of caveolin-1 and -3 is not altered in both global ROCK1 deficient mice and cardiomyocyte-specific ROCK1 knockout mice, indicating the change is merely in caveolar structure and protein distribution, not targeting on protein expression; (2) ROCK1 deficiency is beneficial to preventing caveolae downregulation and preserving caveolar β-adrenergic signaling molecules therefore rescuing the defective β-adrenergic response in cardiomyocytes overexpressing Gαq; (3) In cardiomyocytes and adipocytes, ROCK1 deficiency increases IR activation in caveolae resulting in increased insulin signaling. This phenotype is linked to the increased caveolin levels in caveolae, which most likely contribute to the enhanced interactions among signaling molecules and increased IR activation in caveolae; (4) In MEFs, ROCK1 deficiency increases the ability of maintaining PM integrity after mechanical or chemical disruptions. Together, these results demonstrate an important role for ROCK1 in regulating caveolae plasticity and multiple functions of caveolae under physiopathological conditions. These four major points are discussed below in more details.

4.1 | ROCK1 regulates the organization of caveolar microdomains

Although a physical association between caveolae and the submembrane actin cytoskeleton has been well-established and an excessive formation of stress fibers has been shown to increase PM tension and caveolae flattening,[24,25,49] whether ROCK1 plays a significant role in this process has not been evaluated, especially under physiopathological conditions. Our observation that a pool of RhoA and ROCK1 is localized in the caveolar fractions of cardiac tissues is consistent with the previous studies reporting that RhoA and ROCK1 can physically interact with caveolin-1[50–52] or caveolae can activate RhoA/ROCK through regulating upstream regulators of RhoA.[53,54] Given that a very small pool of ROCK1 is localized in the caveolar fractions, ROCK1 may regulate caveolae organization through several mechanisms. First, caveolar ROCK1 could contribute to the submembrane actin cytoskeleton remodeling and negatively regulate the number of caveolae and clusters. Second, global actin cytoskeleton remodeling controlled by ROCK1 could increase PM tension and negatively regulate the number of caveolae and clusters. Both mechanisms are supported by the literature on the mechanistic interplay between caveolae and actin cytoskeleton.[24,25,49] On the one hand, caveolae localized RhoA/ROCK pathway can be activated by caveolin-1 resulting in actin cytoskeleton remodeling contributing to mechanotransduction at the interface between cytoskeleton and extracellular matrix in response to different stimuli.[50–54] On the other hand, excessive global actin polymerization can increase PM tension and induce caveolae flattening.[24,25,49] Moreover, we previously observed that ROCK1 targets MLC phosphorylation and cortical actomyosin ring formation in MEFs in response to doxorubicin treatment or serum starvation supporting a

role for ROCK1 in regulating PM tension.[17–20] In ROCK1-deficient MEFs, cortical translocation of phosphorylated MLC from central stress fibers was reduced resulting in reduced peripheral actomyosin contraction, cell shrinkage and detachment in response to doxorubicin treatment or serum starvation.[17–20] Collectively, our current findings and other studies support a role for ROCK1 as an important regulator of submembrane actin cytoskeleton, PM tension, caveolae density and clusters in cardiomyocytes, adipocytes and MEFs. The results thus contribute to the expanding list of the regulators of submembrane actin cytoskeleton associated with caveolae, including RhoA and one of its downstream effector mDia1, which produces actin filaments by nucleation and polymerization.[24,25,49] Previous studies and our current results suggest that both RhoA/ROCK1-mediated actomyosin contraction and RhoA/mDia-mediated actin polymerization contribute to the interplay between submembrane actin cytoskeleton and caveolae in regulating the organization of caveolae and consequently their functions.

4.2 | ROCK1 deficiency preserves caveolar compartmentalization of signaling molecules in pathological cardiac hypertrophy and enhances caveolae-mediatedcardioprotectivesignaling

Although the cardiac-specific overexpressing Gαq transgenic mouse model has previously been well-studied as a genetic pathological cardiac hypertrophy model,[10,13,27,28,55] the caveolar subcellular remodeling has not been investigated in this model. Motivated by the our previous observations that ROCK1 deficiency prevents downregulation of AC5/6 protein expression without making changes in their mRNA levels and rescues altered β-adrenergic response in the Gαq transgenic mouse model,[10,13] we further investigated the underlying mechanisms and discovered that ROCK1 deficiency enhances cardioprotective effects mediated by caveolar microdomains. We detected, in subcellular fractionations using discontinuous sucrose gradient centrifugation, the alterations of β-adrenergic signaling molecules in Gαq overexpressing cardiomyocytes are more notable in caveolar fractions than that appeared in ventricular homogenates via protein study: (1) the caveolar level of βAR1 is reduced without a decrease in its total protein level; (2) the caveolar level of AC5/6 is more prominently reduced than their total protein level (about 65% vs. 45% reduction). This prominent reduction of β-adrenergic signaling components in caveolae is expected to disrupt the compartmentation of the cAMP signal in β-adrenergic responding.[56,57] This mechanism mediated by ROCK1/F-actin/caveolae/βARs-Gαs-ACs is consistent with the previous studies demonstrating the contribution of F-actin in regulating caveolar localization of βARs-Gαs-ACs in adult rat and mouse cardiomyocytes.[40] These results also fit well with the growing literature that caveolar microdomains play important roles in cardioprotection in heart diseases including pathological cardiac hypertrophy through two major mechanisms such as compartmentalization of signaling molecules and mechanoprotection.[39,47,48,58,59] In this regard, studies using caveolin-3 knockout mice and cardiac-specific overexpressing caveolin-3 mice have established the link between caveolae and hypertrophy as well as multiple cardioprotective functions of the signaling pathways associated with caveolae including β-adrenergic signaling and PI3K/Akt-mediated survival pathway.[38,60–62]

In addition to the Gαq overexpressing model of pathological hypertrophy, we previously found that ROCK1 deficiency reduces cardiac remodeling in several other pathological models including pressure overload by transverse aortic constriction and doxorubicin-induced cardiotoxicity.[9–14] The protective molecular mechanisms associated with ROCK1 deficiency were found to be different in each of these pathological conditions. For example, increased Akt activation, which is known to play a central role in cardiac protection, was noted in ROCK1 deficient pressure-overloaded hearts.[9,11] In addition, improved autophagy flux through reducing Beclin-1 phosphorylation contributes to ROCK1 deficiency-mediated cardioprotection in doxorubicin cardiotoxicity.[14] The present study demonstrates a common cellular and molecular mechanism for cardioprotection observed in ROCK1-deficient mice through enhancing cardioprotective mechanisms of caveolar microdomains, which include the activation of Akt-mediated survival pathway, preservation of β-adrenergic signaling, and improved autophagic function.[24,25,47,48] It is worth noting that this mechanism mediated by ROCK1/F-actin/caveolae can be extended to other cell types in the heart including endothelial cells and fibroblasts. This is supported by the facts that some caveolar signaling molecules enriched in ROCK1 deficient Gαq overexpressing hearts including caveolin-1 and eNOS are predominantly expressed in endothelial cells. Our findings support the concept that ROCK1 deficiency in cardiomyocytes and non-cardiomyocytes improves cardioprotective mechanisms of caveolar microdomains in pathological cardiac hypertrophy and transition to heart failure.

4.3 | ROCK1 deficiency enhances caveolar IR activation

In supporting that the mechanism mediated by ROCK1/F-actin/caveolae can be extended to other cell types, we confirmed that IR tyrosine phosphorylation is increased

in caveolar microdomains of ROCK1 deficient cardiomyocytes, adipocytes and MEFs. In ROCK1-deficient adipocytes and MEFs, we previously reported that increased insulin signaling is due to increased IR tyrosine phosphorylation which in turn promotes downstream signaling pathways of insulin, including IRS1/PI3K/Akt signaling, but how ROCK1 regulates IR tyrosine phosphorylation in response to insulin has not been defined.[21] The present study provides a common mechanism such as the increased caveolar IR tyrosine phosphorylation in these ROCK1 deficient cells resulting in the increased insulin signaling. There are several potential explanations for the increased caveolar IR tyrosine phosphorylation in these ROCK1 deficient cells. First, the increased caveolar IR tyrosine phosphorylation is likely through direct stimulation of IR kinase activity by increased caveolin levels in caveolar microdomains in a synergistic manner with insulin. In this regard, previous studies have implicated caveolins in regulating IR activity, stability, and localization to caveolae.[41–43,63–65] For example, IR activation is attenuated in caveolin-3 deficient skeletal muscle tissues without affecting IR protein level and its caveolar localization supporting that caveolin-3 directly enhances IR activation in skeletal muscles.[63] In cardiomyocytes, IR also directly interacts with caveolin-3 and caveolin-3 haploinsufficiency reduces insulin signaling without affecting IR protein levels.[41] In adipocytes, caveolin-1 directly interacts with and stabilizes IR in caveolae as in caveolin-1 deficient adipocytes, the IR protein levels decrease by 90% even with normal mRNA expression.[64] In the present study, we observed increased IR tyrosine phosphorylation without affecting IR protein expression in ROCK1 deficient cardiomyocytes, adipocytes and MEFs, suggesting that increased caveolin-1 and -3 levels in caveolar microdomains in these ROCK1 deficient cells do not further increase IR level, but its activation. Second, caveolar PTP1B activity, which dephosphorylates IR tyrosine residues, may be reduced in ROCK1 deficient cells. In this regard, ROCK inhibitor, Y27632, reduces PTP1B activity in human blood–brain barrier cells.[66] Our findings are thus compatible with a novel mechanism mediated by ROCK1/F-actin/caveolae/IR in regulating insulin signaling.

This mechanism validated in ROCK1-deficient cardiomyocytes, adipocytes, and MEFs may not be extended to all cell types. For instance, in skeletal muscles, deficiency of ROCK1 impairs insulin-stimulated IRS1 phosphorylation without affecting IR activation.[29] It is interesting to note that ROCK1 protein level in skeletal muscle is at least 10-fold lower than in cardiac muscle (unpublished observations), suggesting that ROCK1 expression/activity in caveolar microdomains and globally in skeletal muscles may be much lower than that in cardiomyocytes and therefore not enough to contribute to the regulation of caveolar density, clusters, and caveolin-3 levels, as well as IR activation in caveolar microdomains. Further studies are needed to determine whether ROCK1 regulates caveolar structure and functions in other cell types, especially in those with high abundance of caveolae and high expression of ROCK1. Of note, regarding the impact of ROCK activity on insulin signaling, multiple mechanisms have been described including actin-cytoskeleton dependent mechanism or direct interactions of ROCKs with IR signaling components.[67] While our findings point to the importance of ROCK1-mediated actin cytoskeleton remodeling on regulating caveolar IR activation, other studies support a role of ROCK1-mediated actin cytoskeleton dynamics in regulating IRS1 phosphorylation and insulin-dependent glucose transport in cultured adipocytes and muscle cells.[68] It is thus possible that ROCK1-mediated actin cytoskeleton remodeling regulates IR signaling at multiple levels in a cell-type and tissue-dependent manner.

4.4 | ROCK1 deficiency enhances cell membrane repairing

In addition to the enhanced caveolar signal transduction, another important protective effect observed in ROCK1-deficient cells is improved PM repair ability, which is consistent with the well-established function of caveolae in mechanoprotection.[46] We observed that ROCK1 deficiency in MEFs increases membrane resealing ability following mechanical injury of PM (Figure 8). This protective mechanism, possibly mediated by increased caveolar and total levels of caveolin-1 in ROCK1-deficient MEFs, may be extended to other cell types including cardiomyocytes and adipocytes as they are mechanically stressed cells and ROCK1 deficiency in these cells also increases caveolar density and clusters. The PM is the first line of a cell's defense against extracellular stresses, including mechanical and oxidative stresses. PM rupture and consequently loss of PM integrity are key steps in cell death via necrosis. Increased caveolar density and clusters in ROCK1-deficient cells could preserve membrane integrity through two major mechanisms.[24,25] First, increased caveolar density and clusters could protect PM from rupture by increasing membrane reservoirs and reducing the tension at the PM. One important function of caveolae is to serve as membrane reservoirs to buffer increases in membrane tension by changing their curvature, which can range from the classical invaginated form to fully flattened.[24,25] Second, increased caveolar density and clusters could contribute to the enhanced wound repair ability of these cells to maintain membrane integrity. It has been shown that caveolae play an effective role in membrane repair through removing wounded membrane

by caveolar internalization and lysosomal degradation[69,70] and caveolar clusters serve as an intermediate stage during caveolar endocytosis facilitating the removal of PM wounds.[24,25,69,70] These two mechanisms possibly work together providing mechanoprotection to ROCK1-deficient cardiomyocytes, adipocytes and MEFs.

It is worth mentioning that ROCK1 deficiency in MEFs preserves membrane integrity following co-treatment of mechanical injury and oxidative damage of PM induced by doxorubicin. The anthracyclines, primarily doxorubicin, are among the most widely used and successful drugs to treat a wide spectrum of hematologic malignancies and solid tumors but their cumulative and dose-dependent cardiotoxicity has been the major concern of oncologists for decades.[71,72] Our previous studies support the notion that ROCK1 represents a potential therapeutic target in preventing doxorubicin-induced heart failure[14] and cytotoxicity.[17–20] Hence, the preservation of membrane integrity mediated by ROCK1 deficiency could be due to the reduced ROS production,[19,20] reduced susceptibility of PM to mechanical damages and improved PM repair ability.

4.5 | Does ROCK2 contribute to the regulation of caveolar microdomain organization?

As shown in Figure 1B, ROCK2 distribution pattern on sucrose density gradient is similar to that of RhoA and ROCK1, which arises a question whether it plays a similar or different role compared to ROCK1. While future studies using conditional ROCK2 deficient mice or cells are needed to address this question, our previous data suggest that ROCK2 may play a different role compared to ROCK1 in cardiomyocytes, adipocytes and MEFs. We have reported that ROCK isoforms play different roles in regulating insulin signaling and actin cytoskeleton organizations in adipocytes[21,30,67] and MEFs.[17,18] Specifically, different from ROCK1-deficient adipose tissues, insulin-stimulated IR activation was not increased the adipose tissues of ROCK2$^{+/-}$ mice, in which increased insulin signaling was mediated through downstream increased IRS1-mediated PI3K activation.[30] In MEFs, ROCK1 targets MLC2 phosphorylation and peripheral actomyosin contraction, whereas ROCK2 targets both peripheral actomyosin contraction and central stress fiber stability through regulating both MLC and cofilin phosphorylation.[17,18] In cardiomyocytes, we showed a compensatory ROCK1 overactivation in the conditional cardiomyocyte-specific ROCK2 knockout hearts, resulting in different, even opposite, effects on endogenous ROCK activity and cardiac remodeling compared to conditional cardiomyocyte-specific ROCK1 knockout hearts,[31] therefore conditional cardiomyocyte-specific double ROCK KO mice should be used to determine the effects of total loss of ROCKs on caveolar microdomain organization. Of note, the mouse and cell culture models are available for future investigation on the contribution of ROCK2 and total ROCK activity to caveolar microdomain organizations.

In summary, the present study demonstrates an important role for ROCK1 in regulating caveolae plasticity in cardiomyocytes, adipocytes and MEFs in which ROCK1 deficiency increases caveolar density and clusters. In pathological cardiac hypertrophy, this subcellular effect of ROCK1 deficiency is associated with caveolar enriched signal transductions including the preservation of caveolar β-adrenergic signaling and compartmentation of cAMP production. In addition, this effect is correlated with increased caveolar IR activation and consequently improved insulin signaling in cardiomyocytes, adipocytes and MEFs. Finally, this effect is concurrent with increased mechanoprotection through enhancing the ability of maintaining PM integrity following mechanical and oxidative disruption of PM in MEFs. These observations provide a noteworthy molecular insight into the beneficial effects linking to ROCK1 deletion through enhancing caveolae-mediated protective effects in cardiomyocytes, adipocytes, and MEFs under physiopathological conditions.

AUTHOR CONTRIBUTIONS

Jianjian Shi and Lei Wei contributed to the idea for the article, designed and performed research, analyzed data, and wrote the article. Jianjian Shi and Lei Wei agreed with the content of this manuscript and have approved the manuscript before submission.

ACKNOWLEDGMENTS

We thank Dr. Yu Yang, Mr. Lumin Zhang, and Ms. Michelle Surma for technical help. This work was supported by National Institutes of Health grants HL151480 (to L.W. and J.S.), CA263470 (to Dr. Reuben Kapur and J.S.), HL107537 (to L.W.), HL134599 (to L.W.), Riley Children's Foundation (RCF) (to J.S. and to L.W.), and the Indiana Clinical and Translational Sciences Institute (CTSI) (to J.S.).

DISCLOSURES

The authors have no conflicts of interest to declare that are relevant to the content of this article.

DATA AVAILABILITY STATEMENT

The data that support the findings of this study are available in the methods and/or supplementary material of this article.

ETHICS STATEMENT

All animal experiments were conducted in accordance with the National Institutes of Health "Guide for the Care and Use of Laboratory Animals" and were approved by the Institutional Animal Care and Use Committee at Indiana University School of Medicine.

ORCID

Jianjian Shi https://orcid.org/0000-0001-8232-6976
Lei Wei https://orcid.org/0000-0003-3528-9687

REFERENCES

1. Matsui T, Amano M, Yamamoto T, et al. Rho-associated kinase, a novel serine/threonine kinase, as a putative target for small GTP binding protein Rho. *EMBO J*. 1996;15:2208-2216.
2. Ishizaki T, Maekawa M, Fujisawa K, et al. The small GTP-binding protein Rho binds to and activates a 160 kDa Ser/Thr protein kinase homologous to myotonic dystrophy kinase. *EMBO J*. 1996;15:1885-1893.
3. Nakagawa O, Fujisawa K, Ishizaki T, Saito Y, Nakao K, Narumiya S. ROCK-I and ROCK-II, two isoforms of Rho-associated coiled-coil forming protein serine/threonine kinase in mice. *FEBS Lett*. 1996;392:189-193.
4. Amano M, Chihara K, Kimura K, et al. Formation of actin stress fibers and focal adhesions enhanced by Rho-kinase. *Science*. 1997;275:1308-1311.
5. Kimura K, Ito M, Amano M, et al. Regulation of myosin phosphatase by Rho and Rho-associated kinase (Rho-kinase). *Science*. 1996;273:245-248.
6. Leung T, Chen XQ, Manser E, Lim L. The p160 RhoA-binding kinase ROK alpha is a member of a kinase family and is involved in the reorganization of the cytoskeleton. *Mol Cell Biol*. 1996;16:5313-5327.
7. Maekawa M, Ishizaki T, Boku S, et al. Signaling from Rho to the actin cytoskeleton through protein kinases ROCK and LIM-kinase. *Science*. 1999;285:895-898.
8. Arber S, Barbayannis FA, Hanser H, et al. Regulation of actin dynamics through phosphorylation of cofilin by LIM-kinase. *Nature*. 1998;393:805-809.
9. Zhang YM, Bo J, Taffet GE, et al. Targeted deletion of ROCK1 protects the heart against pressure overload by inhibiting reactive fibrosis. *FASEB J*. 2006;20:916-925.
10. Shi J, Zhang YW, Summers LJ, Dorn GW 2nd, Wei L. Disruption of ROCK1 gene attenuates cardiac dilation and improves contractile function in pathological cardiac hypertrophy. *J Mol Cell Cardiol*. 2008;44:551-560.
11. Chang J, Xie M, Shah VR, et al. Activation of Rho-associated coiled-coil protein kinase 1 (ROCK-1) by caspase-3 cleavage plays an essential role in cardiac myocyte apoptosis. *Proc Natl Acad Sci USA*. 2006;103:14495-14500.
12. Shi J, Zhang L, Wei L. Rho-kinase in development and heart failure: insights from genetic models. *Pediatr Cardiol*. 2011;32:297-304.
13. Shi J, Zhang YW, Yang Y, Zhang L, Wei L. ROCK1 plays an essential role in the transition from cardiac hypertrophy to failure in mice. *J Mol Cell Cardiol*. 2010;49:819-828.
14. Shi J, Surma M, Wei L. Disruption of ROCK1 gene restores autophagic flux and mitigates doxorubicin-induced cardiotoxicity. *Oncotarget*. 2018;9:12995-13008.
15. Yang X, Li Q, Lin X, et al. Mechanism of fibrotic cardiomyopathy in mice expressing truncated Rho-associated coiled-coil protein kinase 1. *FASEB J*. 2012;26:2105-2116.
16. Rikitake Y, Oyama N, Wang CY, et al. Decreased perivascular fibrosis but not cardiac hypertrophy in ROCK1+/− haploinsufficient mice. *Circulation*. 2005;112:2959-2965.
17. Shi J, Wu X, Surma M, et al. Distinct roles for ROCK1 and ROCK2 in the regulation of cell detachment. *Cell Death Dis*. 2013;4:e483.
18. Shi J, Surma M, Zhang L, Wei L. Dissecting the roles of ROCK isoforms in stress-induced cell detachment. *Cell Cycle*. 2013;12:1492-1500.
19. Surma M, Handy C, Chang J, Kapur R, Wei L, Shi J. ROCK1 deficiency enhances protective effects of antioxidants against apoptosis and cell detachment. *PLoS ONE*. 2014;9:e90758.
20. Wei L, Surma M, Gough G, et al. Dissecting the mechanisms of doxorubicin and oxidative stress-induced cytotoxicity: the involvement of actin cytoskeleton and ROCK1. *PLoS ONE*. 2015;10:e0131763.
21. Lee SH, Huang H, Choi K, et al. ROCK1 isoform-specific deletion reveals a role for diet-induced insulin resistance. *Am J Physiol Endocrinol Metab*. 2014;306:E332-E343.
22. Parton RG, Kozlov MM, Ariotti N. Caveolae and lipid sorting: shaping the cellular response to stress. *J Cell Biol*. 2020;219:e201905071.
23. Parton RG, McMahon KA, Wu Y. Caveolae: formation, dynamics, and function. *Curr Opin Cell Biol*. 2020;65:8-16.
24. Echarri A, Del Pozo MA. Caveolae—mechanosensitive membrane invaginations linked to actin filaments. *J Cell Sci*. 2015;128:2747-2758.
25. Del Pozo MA, Lolo FN, Echarri A. Caveolae: mechanosensing and mechanotransduction devices linking membrane trafficking to mechanoadaptation. *Curr Opin Cell Biol*. 2021;68:113-123.
26. Agah R, Frenkel PA, French BA, Michael LH, Overbeek PA, Schneider MD. Gene recombination in postmitotic cells. Targeted expression of Cre recombinase provokes cardiac-restricted, site-specific rearrangement in adult ventricular muscle in vivo. *J Clin Invest*. 1997;100:169-179.
27. Adams JW, Sakata Y, Davis MG, et al. Enhanced Galphaq signaling: a common pathway mediates cardiac hypertrophy and apoptotic heart failure. *Proc Natl Acad Sci USA*. 1998;95:10140-10145.
28. D'Angelo DD, Sakata Y, Lorenz JN, et al. Transgenic Galphaq overexpression induces cardiac contractile failure in mice. *Proc Natl Acad Sci USA*. 1997;94:8121-8126.
29. Lee DH, Shi J, Jeoung NH, et al. Targeted disruption of ROCK1 causes insulin resistance in vivo. *J Biol Chem*. 2009;284:11776-11780.
30. Wei L, Surma M, Yang Y, Tersey S, Shi J. ROCK2 inhibition enhances the thermogenic program in white and brown fat tissue in mice. *FASEB J*. 2020;34:474-493.
31. Shi J, Surma M, Yang Y, Wei L. Disruption of both ROCK1 and ROCK2 genes in cardiomyocytes promotes autophagy and reduces cardiac fibrosis during aging. *FASEB J*. 2019;33:7348-7362.
32. Shi J, Zhang L, Zhang YW, Surma M, Mark Payne R, Wei L. Downregulation of doxorubicin-induced myocardial apoptosis accompanies postnatal heart maturation. *Am J Physiol Heart Circ Physiol*. 2012;302:H1603-H1613.
33. Ostrom RS, Insel PA. Methods for the study of signaling molecules in membrane lipid rafts and caveolae. *Methods Mol Biol*. 2006;332:181-191.

34. Yamada E. The fine structure of the gall bladder epithelium of the mouse. *J Biophys Biochem Cytol*. 1955;1:445-458.
35. Palade GE. The fine structure of blood capilaries. *J Appl Phys*. 1953;24:1424-1436.
36. Williams TM, Lisanti MP. The Caveolin genes: from cell biology to medicine. *Ann Med*. 2004;36:584-595.
37. Pugach EK, Richmond PA, Azofeifa JG, Dowell RD, Leinwand LA. Prolonged Cre expression driven by the alpha-myosin heavy chain promoter can be cardiotoxic. *J Mol Cell Cardiol*. 2015;86:54-61.
38. Woodman SE, Park DS, Cohen AW, et al. Caveolin-3 knockout mice develop a progressive cardiomyopathy and show hyperactivation of the p42/44 MAPK cascade. *J Biol Chem*. 2002;277:38988-38997.
39. Wei EQ, Sinden DS, Mao L, Zhang H, Wang C, Pitt GS. Inducible Fgf13 ablation enhances caveolae-mediated cardioprotection during cardiac pressure overload. *Proc Natl Acad Sci USA*. 2017;114:E4010-E4019.
40. Head BP, Patel HH, Roth DM, et al. Microtubules and actin microfilaments regulate lipid raft/caveolae localization of adenylyl cyclase signaling components. *J Biol Chem*. 2006;281:26391-26399.
41. Gustavsson J, Parpal S, Karlsson M, et al. Localization of the insulin receptor in caveolae of adipocyte plasma membrane. *FASEB J*. 1999;13:1961-1971.
42. Talukder MA, Preda M, Ryzhova L, Prudovsky I, Pinz IM. Heterozygous caveolin-3 mice show increased susceptibility to palmitate-induced insulin resistance. *Physiol Rep*. 2016;4:e12736.
43. Haddad D, Al Madhoun A, Nizam R, Al-Mulla F. Role of Caveolin-1 in diabetes and its complications. *Oxidative Med Cell Longev*. 2020;2020:9761539.
44. Mellgren RL, Zhang W, Miyake K, McNeil PL. Calpain is required for the rapid, calcium-dependent repair of wounded plasma membrane. *J Biol Chem*. 2007;282:2567-2575.
45. Corrotte M, Castro-Gomes T, Koushik AB, Andrews NW. Approaches for plasma membrane wounding and assessment of lysosome-mediated repair responses. *Methods Cell Biol*. 2015;126:139-158.
46. Cheng JPX, Nichols BJ. Caveolae: one function or many? *Trends Cell Biol*. 2016;26:177-189.
47. An Z, Tian J, Zhao X, et al. Regulation of cardiovascular and cardiac functions by caveolins. *FEBS J*. 2023. doi:10.1111/febs.16798
48. Tian J, Popal MS, Huang R, et al. Caveolin as a novel potential therapeutic target in cardiac and vascular diseases: a mini review. *Aging Dis*. 2020;11:378-389.
49. Sotodosos-Alonso L, Pulgarin-Alfaro M, Del Pozo MA. Caveolae mechanotransduction at the interface between cytoskeleton and extracellular matrix. *Cell*. 2023;12:942.
50. Kawamura S, Miyamoto S, Brown JH. Initiation and transduction of stretch-induced RhoA and Rac1 activation through caveolae: cytoskeletal regulation of ERK translocation. *J Biol Chem*. 2003;278:31111-31117.
51. Rashid-Doubell F, Tannetta D, Redman CW, Sargent IL, Boyd CA, Linton EA. Caveolin-1 and lipid rafts in confluent BeWo trophoblasts: evidence for Rock-1 association with caveolin-1. *Placenta*. 2007;28:139-151.
52. Taggart MJ, Leavis P, Feron O, Morgan KG. Inhibition of PKCalpha and rhoA translocation in differentiated smooth muscle by a caveolin scaffolding domain peptide. *Exp Cell Res*. 2000;258:72-81.
53. Yang B, Radel C, Hughes D, Kelemen S, Rizzo V. p190 Rhogtpase-activating protein links the beta1 integrin/caveolin-1 mechanosignaling complex to RhoA and actin remodeling. *Arterioscler Thromb Vasc Biol*. 2011;31:376-383.
54. Hetmanski JHR, de Belly H, Busnelli I, et al. Membrane tension orchestrates rear retraction in matrix-directed cell migration. *Dev Cell*. 2019;51:460-475.e410.
55. Dorn GW 2nd, Tepe NM, Wu G, Yatani A, Liggett SB. Mechanisms of impaired beta-adrenergic receptor signaling in G(alphaq)-mediated cardiac hypertrophy and ventricular dysfunction. *Mol Pharmacol*. 2000;57:278-287.
56. Bhogal NK, Hasan A, Gorelik J. The development of compartmentation of cAMP signaling in cardiomyocytes: the role of T-tubules and caveolae microdomains. *J Cardiovasc Dev Dis*. 2018;5:25.
57. Insel PA, Head BP, Ostrom RS, et al. Caveolae and lipid rafts: G protein-coupled receptor signaling microdomains in cardiac myocytes. *Ann N Y Acad Sci*. 2005;1047:166-172.
58. Pradhan BS, Proszynski TJ. A role for caveolin-3 in the pathogenesis of muscular dystrophies. *Int J Mol Sci*. 2020;21:8736.
59. Markandeya YS, Phelan LJ, Woon MT, et al. Caveolin-3 overexpression attenuates cardiac hypertrophy via inhibition of T-type Ca^{2+} current modulated by protein kinase Calpha in cardiomyocytes. *J Biol Chem*. 2015;290:22085-22100.
60. Horikawa YT, Panneerselvam M, Kawaraguchi Y, et al. Cardiac-specific overexpression of caveolin-3 attenuates cardiac hypertrophy and increases natriuretic peptide expression and signaling. *J Am Coll Cardiol*. 2011;57:2273-2283.
61. Tsutsumi YM, Horikawa YT, Jennings MM, et al. Cardiac-specific overexpression of caveolin-3 induces endogenous cardiac protection by mimicking ischemic preconditioning. *Circulation*. 2008;118:1979-1988.
62. Wright PT, Nikolaev VO, O'Hara T, et al. Caveolin-3 regulates compartmentation of cardiomyocyte beta2-adrenergic receptor-mediated cAMP signaling. *J Mol Cell Cardiol*. 2014;67:38-48.
63. Oshikawa J, Otsu K, Toya Y, et al. Insulin resistance in skeletal muscles of caveolin-3-null mice. *Proc Natl Acad Sci USA*. 2004;101:12670-12675.
64. Cohen AW, Razani B, Wang XB, et al. Caveolin-1-deficient mice show insulin resistance and defective insulin receptor protein expression in adipose tissue. *Am J Physiol Cell Physiol*. 2003;285:C222-C235.
65. Capozza F, Combs TP, Cohen AW, et al. Caveolin-3 knockout mice show increased adiposity and whole body insulin resistance, with ligand-induced insulin receptor instability in skeletal muscle. *Am J Physiol Cell Physiol*. 2005;288:C1317-C1331.
66. Pinzon-Daza ML, Salaroglio IC, Kopecka J, et al. The cross-talk between canonical and non-canonical Wnt-dependent pathways regulates P-glycoprotein expression in human blood-brain barrier cells. *J Cereb Blood Flow Metab*. 2014;34:1258-1269.
67. Wei L, Shi J. Insight into rho kinase isoforms in obesity and energy homeostasis. *Front Endocrinol (Lausanne)*. 2022;13:886534.
68. Chun KH, Araki K, Jee Y, et al. Regulation of glucose transport by ROCK1 differs from that of ROCK2 and is controlled by actin polymerization. *Endocrinology*. 2012;153:1649-1662.
69. Andrews NW, Almeida PE, Corrotte M. Damage control: cellular mechanisms of plasma membrane repair. *Trends Cell Biol*. 2014;24:734-742.

70. Kitmitto A, Baudoin F, Cartwright EJ. Cardiomyocyte damage control in heart failure and the role of the sarcolemma. *J Muscle Res Cell Motil*. 2019;40:319-333.
71. Zhang YW, Shi J, Li YJ, Wei L. Cardiomyocyte death in doxorubicin-induced cardiotoxicity. *Arch Immunol Ther Exp (Warsz)*. 2009;57:435-445.
72. Shi J, Abdelwahid E, Wei L. Apoptosis in anthracycline cardiomyopathy. *Curr Pediatr Rev*. 2011;7:329-336.

How to cite this article: Shi J, Wei L. ROCK1 deficiency preserves caveolar compartmentalization of signaling molecules and cell membrane integrity. *FASEB BioAdvances*. 2024;6:85-102. doi:10.1096/fba.2024-00015